DISPLAY FEATURES OF A ROOM-TEMPERATURE TWISTED NEMATIC DISPLAY MATERIAL BY DOPING SINGLE-WALLED CARBON NANOTUBES

Bharti Yadav[1, 2], Akash Yadav[1], B. S. Sharma[3], Prashant Kumar Pandey[4], Abhay S. Pandey[5*]

Abstract:

The current study focuses on the optical, dielectric, and electro-optical properties of single-walled carbon nanotubes (SWCNTs) doped in the nematic matrix of a room temperature liquid crystalline material 4-(trans-4′-*n*-hexylcyclohexyl)isothiocyanatobenzene (6CHBT). The nematic liquid crystalline material used in the study is 6CHBT. It has been doped with SWCNTs of diameter ~ 0.8-1.4 nm and length ~100-300 nm. The nematic liquid crystalline material 6CHBT is an ideal base material for displays because of its low viscosity and nematic phase temperature range of 12.5 - 43.0 °C. SWCNTs have been doped in 6CHBT in two different concentrations i.e., 0.01 and 0.02% (weight ratio). For higher concentrations, CNTs were observed to be bundled at different locations. For this reason, higher concentrations were not studied. Using electro-optical and dielectric spectroscopy, the effects of SWCNTs doping on a number of display characteristics, including threshold voltage, dielectric anisotropy, and splay elastic constant, have been investigated. SWCNTs alignment parallel to the nematic direction is supported by the nematic phase. Yet, the SWCNTs enhance the local orientational arrangement of the molecules in the nematic phase. As a result, the inclusion of the SWCNTs significantly lowers the threshold voltage necessary to convert the molecules from planar (bright state) to homeotropic (dark state) shape.

Keywords: SWCNTs, Nematic Displays, 6CHBT, ^{1}H-NMR, ^{13}C-NMR and Display Parameters.

[1]Ph.D. Research Scholar of Lords School of Sciences, Lords University, Chikani, Alwar, Rajasthan, India.
[2]Associate Professor of Physics, Government College, Kanina, Mahendergarh, Haryana, India.
[3]Professor and Pro-Chairperson of Lords University, Chikani, Alwar, Rajasthan, India.
[4]Professor of Physics and Director, Ansal Technical Campus, Lucknow, India.
[5]Associate Professor of Physics, Department of Science, Lucknow Public College of Professional Studies, Vinamra Khand, Gomti Nagar, Lucknow, India.

*Corresponding Author: Dr. Abhay S. Pandey
Associate Professor of Physics, Department of Science, Lucknow Public College of Professional Studies, Vinamra Khand, Gomti Nagar, Lucknow, India. E-mail: abhaypandey.liquidcrystal@gmail.com

Eur. Chem. Bull. **2023**, *12(Special Issue 5), 5698 – 5706*

5698

1. Introduction:

Researchers have become increasingly interested in nanoparticles and nanotubes recently due to their remarkable electrical, optical, and magnetic properties [1]. In certain investigations, nanoparticles have been employed successfully to improve the electrooptical qualities of materials used in liquid crystal displays [2-8]. Most of the time, nanoparticles decreased the threshold voltage (V_{th}) necessary to change the configuration of the molecules from planar to homeotropic. A nematic liquid crystal display material, 5CB, recently had its electro-optical (E-O) characteristics improved by electron beam irradiation [9]. The dielectric anisotropy of the material may be modified to improve the steepness of the transmission-voltage (T-V) curve by employing an appropriate dose of electron beam irradiation; however an increase in the threshold voltage was seen. In the current study, we show that the doping of single-wall carbon nanotubes (SWCNTs) changed the display properties (threshold voltage, dielectric anisotropy, and splay elastic constant) of another room-temperature nematic liquid crystalline material. The substance employed in the investigation is 4-(trans-4'-*n*-hexylcyclohexyl)isothiocyanatobenzene(6CHBT), a nematic liquid crystal. SWCNTs with a diameter of 0.8 to 1.4 nm and a length of 100 to 300 nm have been added to it. Due to its low viscosity and nematic phase temperature range of 12.5–43.0 °C, the nematic liquid crystalline material 6CHBT is a perfect basis material for displays [10].

2. Synthesis and Characterization of a Room Temperature Liquid Crystalline Material 4-(trans-4'-*n*-hexylcyclohexyl)isothiocyanatobenzene (6CHBT):

2.1 Synthesis: The chemical structure of the nematic liquid crystalline material 6CHBT having its low viscosity and nematic phase temperature range of 12.5-43.0 °C is shown in **Figure 1**.
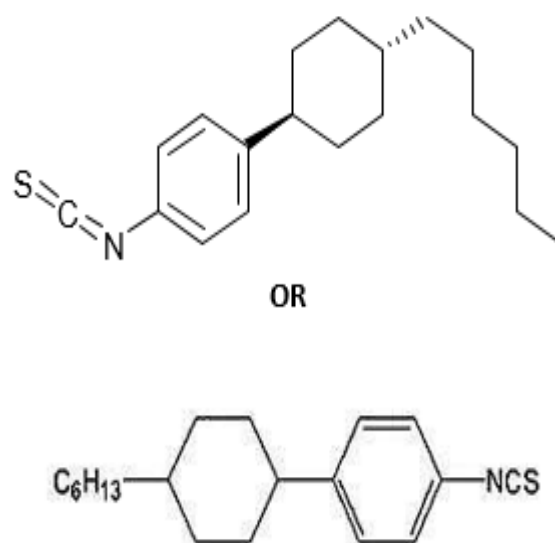

Figure 1: Chemical structure of the synthesized nematic liquid crystalline material 6CHBT.

A portion of 25.8 g (0.1 mole) of 4-(trans-4′-n-hexylcyclohexyl)aniline was dissolved in a mixture of 80 ml benzene and 20 ml hexane, then *7.5* ml (0.1 mole) of carbon disulfide and 15 ml of triethylamine were added and the mixture was left to stand for 45 hours at 0°C. The yellow triethylammonium dithiocarbamate precipitate was filtered off, washed with hexane and dried. The crystalline product was dissolved in 100 ml of chloroform and 15.5 ml of triethylamine was added. The solution was cooled to 0°C and at this temperature 15.5 ml of ethyl chloroformate were added with continuous stirring. Then the mixture was allowed to warm-up to room temperature, when stirring was continued for 1 hour, it was then poured into 500 ml of a 3M hydrochloric acid. The organic layer was separated from the aqueous one, washed with water, dried down and the residue crystallized from ethanol. The yield was 15 g of 6CHBT having the following phase transition points: Cr 12.5°C N 43.0°C I.

Anal. calcd for $C_{19}H_{27}NS$: C = 75.69%, H = 9.03%, N = 4.65%, S = 10.64 %

Found: C = 75.66%, H = 9.09%, N = 4.51%, S = 10.62 %

Eur. Chem. Bull. **2023**, *12(Special Issue 5), 5698 – 5706*
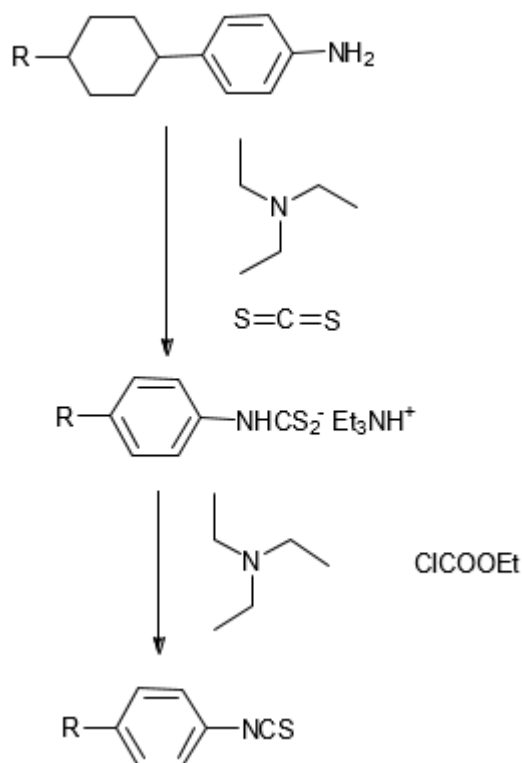
5699

Figure 2: Reaction Method utilized to create the Nematic Liquid Crystalline Substance 6CHBT.

2.2 Characterization: Carbon-13 (C13) nuclear magnetic resonance (most commonly known as carbon-13 NMR spectroscopy or ^{13}C NMR spectroscopy or sometimes simply referred to as carbon NMR) is the application of nuclear magnetic resonance (NMR) spectroscopy to carbon. It is analogous to proton NMR (^{1}H NMR) and allows the identification of carbon atoms in an organic molecule just as proton NMR identifies hydrogen atoms. ^{13}C NMR detects only the ^{13}C isotope. The main carbon isotope, ^{12}C is not detected. Although much less sensitive than ^{1}H NMR spectroscopy, ^{13}C NMR spectroscopy is widely used for characterizing organic and organometallic compounds.
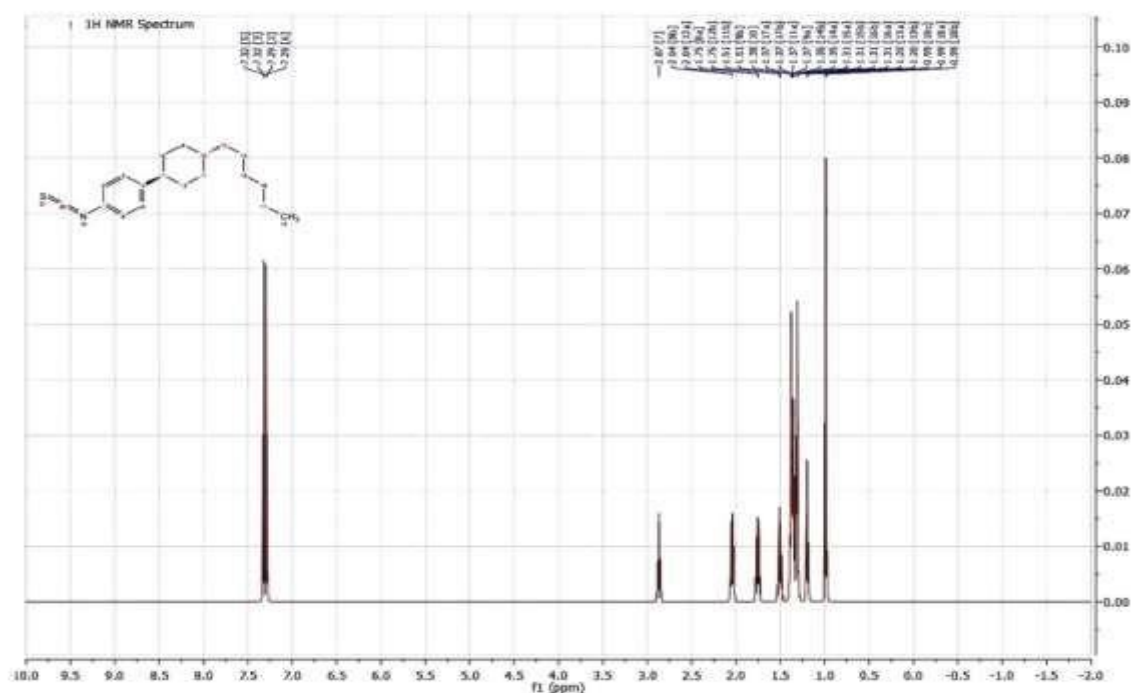

Figure 3: ^{1}H NMR Spectrum of the liquid crystalline substance 6CHBT demonstrates that the molecule was effectively synthesized.
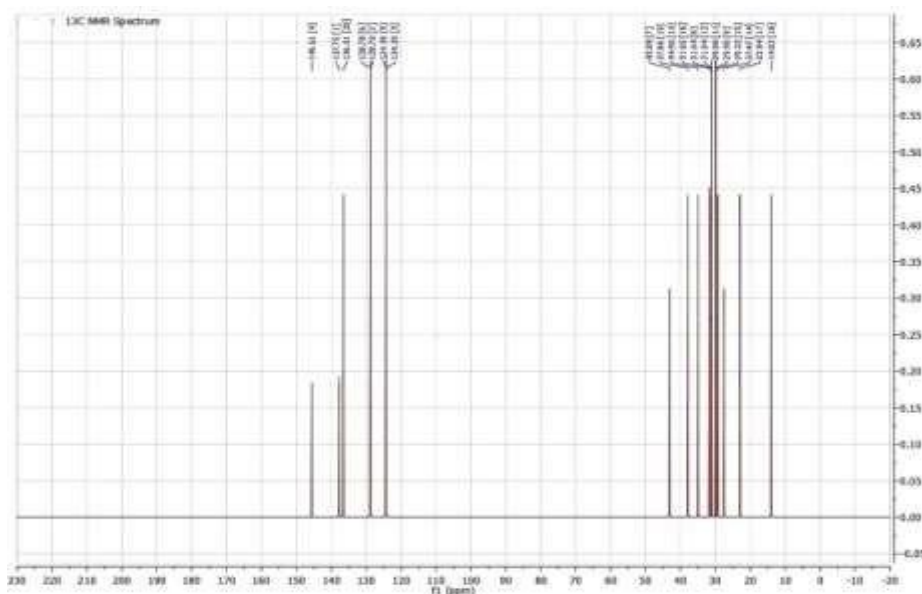
Figure 4: ^{13}C NMR Spectrum of the liquid crystalline substance 6CHBT shows that the compound was synthesized successfully.

3. Experimental Procedures used in Electrical and Electro-Optical Investigation:

To manufacture the cells with electrode spacing (d) of 5 μm, polymer-coated and parallel-rubbed Indium tin oxide (ITO)-coated glass plates with a pre-tilt angle of 1-3° were employed. From Instec in the USA, these cells were bought. In these cells, molecules are arranged parallel to the direction that the glass plates rub against one another. The static value of the transverse component of relative dielectric permittivity ($\varepsilon_\perp'$) was calculated using the same cell. Nevertheless, to produce the cells for the measurement of the longitudinal component of relative dielectric permittivity ($\varepsilon_{||}'$), gold coated glass plates with an additional coating of lecithin were utilized. Using a polarized light microscope and a photo-detector device from Instec, E-O characteristics (T-V curves) were created. Using a six and a half digit multimeter, the photo-voltage (which is proportional to the intensity of the transmitted light) obtained from the photo-detector was recorded. The T-V curve was used to calculate $V_{th.}$. Using an impedance meter (N4L, model PSM-1735) linked with an impedance analyzer interface, dielectric permittivity measurements were collected in the frequency range of 1 Hz to 35 MHz in order to identify further display characteristics. A hot stage with an accuracy of ± 0.1°C (Instec, model HS-1) was used to regulate the sample's temperature. As there are no low- or high-frequency artifacts [11-13] and no dispersion mechanism up to this frequency, the 10 kHz dielectric measurements have been regarded as

the "static" values. The relative dielectric permittivity $\Delta\varepsilon'$ (=$\varepsilon_{||}'$ - $\varepsilon_\perp'$) anisotropy has been determined using this data. Our prior papers [14, 15] provide further information regarding the experimental methods utilized for the dielectric measurements.

4. Results and discussion:

In two distinct concentrations, i.e., 0.01 and 0.02% (weight ratio), SWCNTs have been doped in 6CHBT. A homogeneous distribution of SWCNTs up to 0.02% in the nematic matrix of 6CHBT is confirmed by the optical texture in *Figure 5*. The 6CHBT molecules' improper homeotropic orientations in relation to the SWCNTs are what cause the bright spots to appear in *Figure 5*. CNTs were shown to be bundled in various sites for higher concentrations, nevertheless. Higher concentrations weren't examined due of this. T-V curves for pure and SWCNTs doped 6CHBT samples at 22.0 °C are shown in *Figure 6*. When molecules are aligned in a planar manner at low voltages (V_{th}), a brilliant state is seen. Molecules eventually change to a homeotropic orientation (molecular director normal to the electrode surface) as applied voltage is raised above V_{th}, and dark condition is seen. Switching voltage interval is the voltage needed to shift the intensity from 90% of the maximum value to 10%. The switch voltage interval serves as a gauge for the T-V curve's steepness. *Table 1* contains the threshold voltages that were determined from these T-V curves.

Eur. Chem. Bull. **2023**, *12(Special Issue 5), 5698 – 5706*
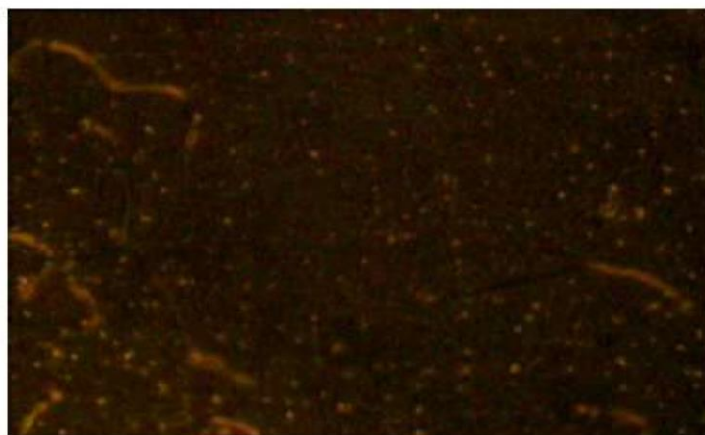
5701

Figure 5: Under homeotropic conditions, the optical texture of 6CHBT doped with 0.02% SWCNT is shown. Bright dots on the dark field of view represent the spread of SWCNTs (due to incorrect homeotropic orientation of 6CHBT molecules surrounding nanotubes).
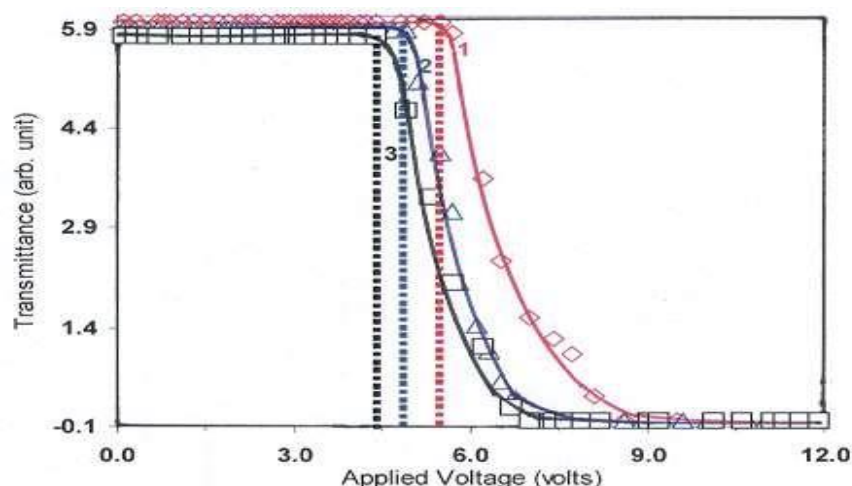

Figure 6: Transmission-voltage (T-V) curves for pure (circles), 0.01% (triangles), and 0.02% (squares) SWCNTs in 6CHBT. The vertical lines indicate threshold voltages.

Table 1: Threshold Voltage (V_{th}), Dielectric Anisotropy (at 10 kHz), Splay Elastic Constant (K_{11}), and Relaxation Frequency (f_r) corresponding to flip-flop motion of molecules along their short axes at 22.0°C.

Name of the Studied Material	V_{th} (volt)	$\Delta\varepsilon'$ ($= \varepsilon_{\parallel}' - \varepsilon_{\perp}'$)	K_{11} (N)	f_r (MHz)
6CHBT	5.5	5.20	1.40×10^{-10}	1.47
6CHBT + 0.01% weight ratio SWCNTs	4.9	6.26	1.37×10^{-10}	1.68
6CHBT + 0.02% weight ratio SWCNTs	4.4	6.97	1.24×10^{-10}	2.93

It is evident from ***Figure 6*** and ***Table 1*** that as SWCNTs doping concentration is increased, V_{th} greatly reduces, which is advantageous from an application standpoint. Due to the doping of SWCNTs, the T-V curve's steepness is also becoming better (see ***Figure 6***).

The following equation describes the threshold voltage:

$$V_{th} = \pi(K_{eff} / \varepsilon_0\Delta\varepsilon')^{1/2}, \qquad (1)$$

where $K_{eff} = [K_{11} + (1/4)(K_{33}-2K_{22})]$ or K_{11} for twisted/parallel cells, respectively. K_{11}, K_{22} and

K_{33} are respectively the splay, twist and bend elastic constants and ε_0 (=8.85 pF/m) is the free space permittivity. The measurements of $\varepsilon_{\parallel}'$ and $\varepsilon_{\perp}'$ [14] outlined previously have been made in order to determine $\Delta\varepsilon'$ and K_{11}. ***Figure 7*** depicts variations in $\varepsilon_{\parallel}'$ and $\varepsilon_{\perp}'$ (and hence $\Delta\varepsilon'=\varepsilon_{\parallel}' - \varepsilon_{\perp}'$) with temperature for both pure and SWCNTs doped 6CHBT samples. ***Figure 7*** demonstrates that $\Delta\varepsilon'$ grows with SWCNTs concentration. By utilizing equation 1 and experimental results for V_{th} and $\Delta\varepsilon'$, K_{11} has been calculated and is shown

Eur. Chem. Bull. **2023**, *12(Special Issue 5), 5698 – 5706*

5702

in **Table 1**. **Table 1** shows that with an increase in the doping concentration of SWCNTs, V_{th} and K_{11} drop while increases. According to the analysis of the optical response (under square pulse), the doping of the SWCNTs causes the time needed for homeotropic to planar switching (τ_{off}) to rise (it is 250 ms for pure 6CHBT compared to 280 and 350 ms for 0.01 and 0.02% SWCNTs doped in 6CHBT, respectively). Due to the fact that τ_{off} is inversely correlated to K_{11} (τ_{off}

K_{11}, where γ is the material's rotational viscosity), and as a result, the presence of SWCNTs in 6CHBT promotes both a rise in τ_{off} and a decrease in K_{11}.

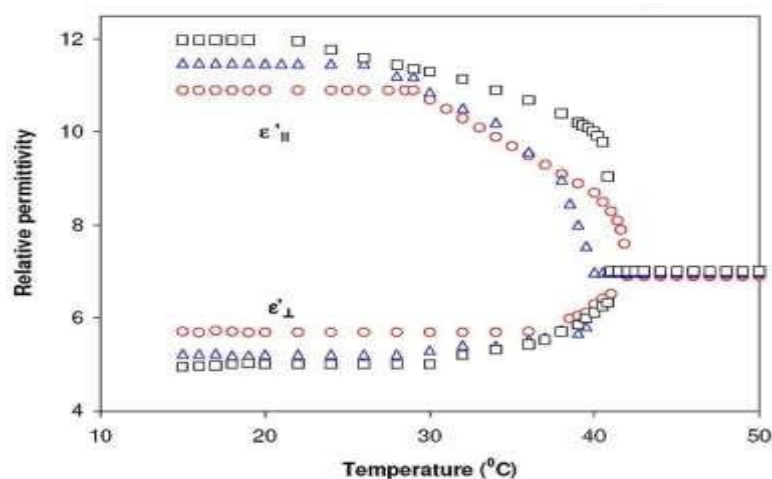Thus, SWCNTs reduce threshold voltage by altering the magnitudes of both $\Delta\varepsilon'$ and K_{11}.

Figure 7: Variations in the longitudinal and transverse components of relative dielectric permittivity ($\varepsilon_{||}'$ and $\varepsilon_{\perp}'$ respectively) and therefore dielectric anisotropy ($\Delta\varepsilon' = \varepsilon_{||}' - \varepsilon_{\perp}'$) with temperature for pure (circles), with 0.01% (triangles) and 0.02% (squares) SWCNTs in 6CHBT.

Using gold-coated glass plates as the cell's electrodes, we measured $\varepsilon_{||}'$ and $\varepsilon_{\perp}'$ as a function of frequency in order to evaluate the impact of SWCNTs at the molecular level has been discovered to be essentially invariant throughout the frequency range from 1 Hz to 10 MHz, indicating that the dielectric relaxation associated with molecule rotation along their long axes occurs much above this frequency. $\varepsilon_{||}'$ reveals a relaxation mechanism in the high frequency range, nevertheless (see **Figure 8**). We connect flip-flop motion of molecules along their short axes to relaxation frequency magnitudes and their temperature dependence (Arrhenius behaviour). The relaxation frequency increases as the SWCNTs' doping concentration increases. Hence, when doping concentration grows, the useful frequency range (below relaxation frequency) for display applications expands.

We now move on to the justification for the observed alterations in the different parameters brought on by the doping of the SWCNTs. SWCNTs have a length between 100 and 300 nm, whereas the molecular length of 6CHBT is about 2.5 nm [10]. As a result, the typical SWCNT length is between 40 and 120 times that of the

6CHBT. Our experiments have corroborated what Dierking et al. [16] stated about nano tubes aligning parallel to the nematic direction when they are scattered in the nematic matrix. In these circumstances, nanotubes will create nano-containers with an average depth that is 40–120 times longer than the length of the 6CHBT molecules. The local short range orientational ordering of the molecules contained between nanotubes will improve because nanotubes are parallel to the nematic director (average direction of the molecules in the nematic phase). This will raise the nematic phase's orientational order parameter (S).
According to Maier and Meier theory [17, 18]

$$\Delta\varepsilon' = \frac{NhF}{\varepsilon_0}\left[\Delta\alpha - \frac{F}{2kT}\mu^2(1-3\cos^2\beta)\right]S \tag{2}$$

In this case, $\Delta\varepsilon'$ is proportional to the macroscale parameters S and N (number of LC molecules per unit volume). When the doping concentration of SWCNTs increases, N is anticipated to decrease, and as a result, $\Delta\varepsilon'$ should decrease. Hence, an increase in $\Delta\varepsilon'$ is only feasible if S rises as a result of the doping of SWCNTs in a way that it outweighs the reducing impact of N. It is not

Eur. Chem. Bull. **2023**, *12(Special Issue 5), 5698 – 5706*

5703

anticipated that SWCNTs would modify any other equation (2) parameters relating to molecular characteristics [17–19]. Hence, the doping of SWCNTs is to blame for the rise in the dielectric anisotropy by increasing the order parameter of the nematic phase. Moreover, the splay elastic constant has decreased due to the presence of SWCNTs between molecules. Also, the number of 6CHBT molecules per unit volume will decrease due to the presence of SWCNTs in the nematic matrix of 6CHBT (which have bigger dimensions than 6CHBT molecules), and this will promote the flip-flop motion of 6CHBT

molecules along their short axes [20, 21]. As a result, relaxation frequency increasing in accordance with the molecules' flip-flop motion about their short axes. The availability of more space marginally outweighs the former impact, despite the fact that the existence of nanotubes in the nematic framework should slow down flip-flop movement about the short axis of the molecules due to their heavier structure than LC molecules.

Though unusual, occurrences like these do occur (see ref. 21 and citations therein).
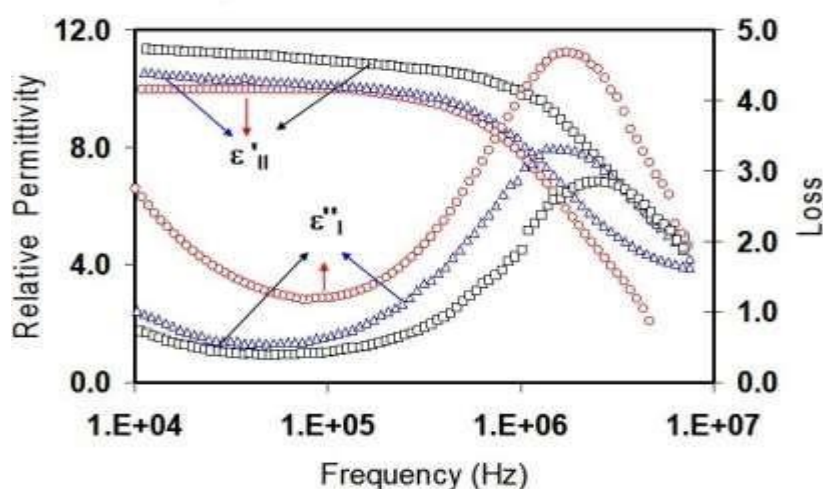

Figure 8: Variations of longitudinal components of relative dielectric permittivity and loss ($\varepsilon_{\parallel}'$ and $\varepsilon_{\parallel}''$) respectively) with frequency for pure (circles), with 0.01% (triangles) and 0.02% (squares) SWCNTs in 6CHBT.
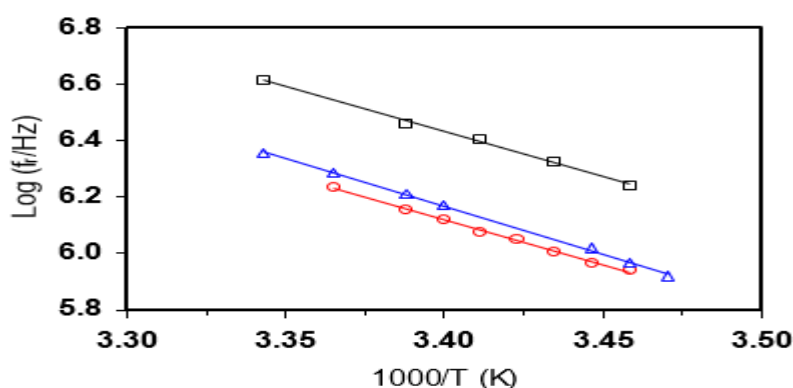

Figure 9: Arrhenius graphs (log of relaxation frequency against temperature inverse) for pure (circles), 0.01% (triangles), and 0.02% (squares) SWCNTs in 6CHBT. Straight line slopes provide activation energy.

Relaxation frequencies follow Arrhenius equation [21]

$$f_r = A\,\exp\,(-E_a/N_A kT) \qquad (3)$$

where E_a is the activation energy associated to the flip-flop motion of molecules along their short

axes, N_A is the Avagadro number, and k is the Boltzman constant. The method of least square fit has been used to determine the slopes of the log (f_r) vs. inverse of temperature plots. Almost identical activation energies (63±2 kJ/mole) have been determined for pure and doped systems using the slopes of straight lines (see **Figure 9**).

Eur. Chem. Bull. **2023**, *12(Special Issue 5), 5698 – 5706*

5704

5. Conclusions:

The following points summarize the experimental results for pure, with 0.01% and 0.02% SWCNTs in 6CHBT.

• The liquid crystalline material 4-(trans-4′-*n*-hexylcyclohexy)isothiocyanatobenzene (6CHBT) have been synthesized at laboratory through standard operating procedure. It was separated out, dried and melting point was recorded on *Toshniwal Electronic Melting Point Apparatus*. Analysis was confirmed by calculating C, H, N, S via mass % of the sample. The ^1H NMR and ^{13}C NMR were recorded which confirms that the compound was successfully synthesized.

• The variations of longitudinal and transverse components of relative permittivity $\varepsilon_{||}'$ and $\varepsilon_{\perp}'$ respectively) and hence dielectric anisotropy ($\Delta\varepsilon' = \varepsilon_{||}' - \varepsilon_{\perp}'$) with temperature increases due to the presence of SWCNTs in the nematic matrix of 6CHBT. Further, it temperature also confirms that all the studied samples i.e. pure; with 0.01% and 0.02% SWCNTs in 6CHBT possess positive dielectric anisotropy.

• The addition of SWCNTs in the nematic matrix of 6CHBT has been shown to reduce the splay elastic constant.

• The threshold voltage needed to change a molecule's conformation from planar (bright state) to homeotropic (dark state) is therefore significantly reduced as a result of these two characteristics.

• The alignment of the SWCNTs parallel to the nematic direction is supported by the nematic matrix. On the other hand, the presence of SWCNTs enhances local orientational ordering of molecules in the nematic phase, most likely as a result of strong van der Waals interactions and a corresponding rise in nematic order parameter.

• The relaxation frequency corresponding to the flip-flop motion of the molecules about their short axes increases. With increase in the doping concentration of SWCNTs, relaxation frequency goes up. Thus usable frequency range (below relaxation frequency) for display applications increases as doping concentration increases.

References:

1. Nanotechnology 2008: Materials, Fabrication, Particles and Characterization, Proc.Nano Science and Technology Institute, Cambridge, MA, USA, (CRC Press, 2008), P. 1-182.
2. S. Kaur, S. P. Singh, A. M. Biradar, A. Choudhary, and K. Sreenivas: Appl. Phys. Lett. 91 (2007) 023120.
3. S. Kumar and H. Bisoyi: Angew. Chem., Int. Ed. 46 (2007) 1501.
4. S. Kumar, S.K. Pal, P. S. Kumar, V. Lakshminarayanan: Soft Matter 3 (2007) 896.
5. Y. Shiraishi, N. Toshima, K. Maeda, H. Yoshikawa, J. Xu, and S. Kobayashi: Appl. Phys. Lett. **81** (2002) 2845.
6. Y. Reznikov, O. Buchnev, and O. Tereshchenko, V. Reshetnyak, A. Glushchenko, and J. West: Appl. Phys. Lett. 82 (2003) 1917.
7. C. I. Cheon, L. Li, A. Glushchenko, J. L. West, Y. Reznikov, J. S. Kim, and D. H. Kim: SID Int. Symp. Dig. Tech. Pap. 36 (2005) 1471.
8. F. Haraguchi, K. Inoue, N. Toshima, S. Kobayashi, and K. Takotoh: Jpn. J. Appl. Phys. 34 (2007) L796.
9. R. Dhar, R. Verma, M. C. Rath, S. K. Sarkar, V. K. Wadhawan, R. Dabrowski, and M. Tykarska: Appl. Phys. Lett. 92 (2008) 014108.
10. P. Sarkar, P. Mandal, S. Paul, R. Paul, R. Dabrowski, and K. Czuprynski: Liq. Cryst. 30 (2003) 507.
11. S. L. Srivastava and R. Dhar: Indian J. Pure Appl. Phys. 29 (1991) 745.
12. R. Dhar: Indian J. Pure Appl. Phys. 42 (2004) 56.
13. M. B. Pandey, R. Dhar, V. K. Agrawal, R. Dabrowski and M. Tykarska: Liq. Cryst. 31 (2004) 973.
14. M. Gupta, R. Dhar, V. K. Agrawal, R. Dabrowski, and M. Tykarska: Phys. Rev. E 72, 021703 (2005).
15. R. Dhar, M. Gupta, V. K. Agrawal, and S. Kumar: Phase Transitions 81 (2008) 459.
16. Dierking, G. Scalia, and P. Morales: J. Appl. Phys. **97** (2005) 044309.

17. W. Maier and G. Meier: Z. Naturforsch 16A (1961) 262.
18. H. Kresse: in Advances in Liquid Crystals, ed. G.H. Brown, (Academic Press, New York, 1983), Vol. 6, P. 109.
19. S.L. Srivastava and R. Dhar: Indian J. Pure Appl. Phys. 37 (1999) 891.
20. D.M.F. Edwards and P.A. Madden: Mol. Phys. 48 (1983) 471.
21. R. Dhar, M. Gupta, V. K. Agrawal, and M. K. Singh: Phase Transitions 81 (2008) 341.

Eur. Chem. Bull. **2023**, *12(Special Issue 5), 5698 – 5706*

5706